Ultra-precise characterization of LCLS hard X-ray focusing mirrors by high resolution slope measuring deflectometry

Frank Siewert,[1,*] Jana Buchheim,[1] Sébastien Boutet,[2] Garth J. Williams,[2] Paul A. Montanez,[2] Jacek Krzywinski,[2] and Riccardo Signorato[3]

[1]Helmholtz Zentrum Berlin, BESSY-II, Institute for Nanometre Optics and Technology, Albert-Einstein-Str. 15, 12489 Berlin, Germany[2] Linac Coherent Light Source, SLAC – National Accelerator Laboratory, 2575 Sand Hill Road, Menlo Park, CA 94025-7015, USA

[3]Bruker ASC GmbH, Friedrich-Ebert-Str. 1, 51429 Bergisch-Gladbach, Germany

[*]frank.siewert@helmholtz-berlin.de

Abstract: We present recent results on the inspection of a first diffraction-limited hard X-ray Kirkpatrick-Baez (KB) mirror pair for the Coherent X-ray Imaging (CXI) instrument at the Linac Coherent Light Source (LCLS). The full KB system – mirrors and holders - was under inspection by use of high resolution slope measuring deflectometry. The tests confirmed that KB mirrors of 350mm aperture length characterized by an outstanding residual figure error of <1 nm rms has been realized. This corresponds to the residual figure slope error of about 0.05µrad rms, unprecedented on such long elliptical mirrors. Additional measurements show the clamping of the mirrors to be a critical step for the final – shape preserving installation of such outstanding optics.

OCIS codes: (340.0340) X-ray optics; (140.2600) Free-electron lasers (FELs); (120.3940) metrology.

References and links

1. E. Debler, and K. Zander, "Ebenheitsmessung an optischen Planflächen mit Autokollimationsfernrohr und Pentagonprisma", PTB Mitteilungen Forschen + Prüfen, Amts und Mitteilungsblatt der Physikalisch Technischen Bundesanstalt, Braunschweig und Berlin, **89**, 339-349 (1979)
2. K. von Bieren, "Pencil beam interferometer for aspheric optical surfaces", Proc. of SPIE **343**, 101-108 (1982)
3. P. Takacs, S. N. Qian and J. Colbert, "Design of a long trace surface profiler", Proc. of SPIE **749**, 59-64 (1987)
4. P. Takacs, S. N. Qian, "Surface Profiling interferometer", US patent No.U4884697, (Dec. 5, 1989)
5. Frank Siewert, Tino Noll, Thomas Schlegel, Thomas Zeschke, and Heiner Lammert, "The Nanometer Optical Component Measuring machine: a new Sub-nm Topography Measuring Device for X-ray Optics at BESSY", AIP Conference Proceedings **705**, 847-850 (2004)
6. H. Lammert, T. Noll, T. Schlegel, F. Siewert, T. Zeschke, "Optisches Messverfahren und Präzisionsmessmaschine zur Ermittlung von Idealformabweichungen technisch polierter Oberflächen", Patent No.: EP 1 585 938 B1 (07.26. 2006)
7. S.G. Alcock, K.J.S. Sawhney, S. Scott, U. Pedersen, R. Walton, F. Siewert, T. Zeschke, T. Noll and H. Lammert, "The Diamond-NOM: A non-contact profiler capable of characterizing optical figure error with sub-nm repeatability", Nucl. Instrum. Meth. A **616**, 224-228 (2010)
8. V.V. Yashchuk, S. Barber, E.E. Domning, J.L. Kirschman, G.Y. Morrison, B.V. Smith, F. Siewert, T. Zeschke, R. Geckler, A. Just, "Sub-microradian surface slope metrology with the ALS Developmental Long Trace Profiler", Nucl. Instrum. Meth. A, **616,** 212-223 (2010)
9. I. Weingärtner, M. Schulz, and C. Elster, "Novel scanning technique for ultra-precise measurement of topography", in "Optical Manufacturing and Testing III", Proc. of SPIE **3782**, 306-317 (1999)

10. R.D. Geckeler, I. Weingärtner, "Sub-nm topography measurement by deflectometry: flatness standard and wafer nanotopography", Proc. of SPIE, **4779**, 1-12 (2002)
11. F. Siewert, J. Buchheim, T. Zeschke, G. Brenner, S. Kapitzki, K. Tiedtke, "Sub-nm accuracy metrology for ultra-precise reflective X-ray optics", Nucl. Instrum. Meth. A **635,** 552-557 (2010)
12. F. Siewert, J. Buchheim, T. Zeschke, "Calibration and characterization of 2nd generation slope measuring profiler", Nucl. Instrum. Meth. A **616**, 119-127 (2010)
13. V. Yashchuk, W. McKinney, T. Warwick, T. Noll, F. Siewert, T. Zeschke, R. Geckeler, "Proposal for a Universal Test Mirror for Characterization of Slope Measuring Instruments", Advances in Metrology for X-Ray and EUV Optics II, Proc. of SPIE, **6704**, 4-16 (2007)
14. R.D. Geckeler, A. Just, M. Krause, V.V. Yashchuk, "Autocollimators for deflectometry: Current status and future progress", Nucl. Instrum. Meth. A **616,** 140-146 (2010)
15. M. Altarelli, R. Brinkmann, M. Chergui, W. Decking, B. Dobson, S. Düsterer, G. Grübel, W. Graeff, H. Graafsma, J. Hajdu, J. Marongos, J. Pflüger, H. Redlin, D. Riley, I. Robson, J. Rossbach, A. Schwarz, K. Tiedtke, T. Tschentscher, I. Vartaniants, H. Wabnitz, H. Weise, R. Wichmann, K. Witte, A. Wolf, M. Wulff, M. Yurkov "The European X-Ray Free Electron Laser – Technical Design Report", DESY, Hamburg, (July 2006)
16. H. Mimura, S. Handa, T. Kimura, H. Yumoto, D. Yamakawa, H. Yokoyama, S. Matsuyama, K. Inagaki, K. Yamamura, Y. Sano, K. Tamasaku, Y. Nishino, M. Yabashi, T. Ishikawa, K. Yamauchi, "Breaking the 10 nm barrier in hard-X-ray focusing", Nature Physics **1457**, 1-4 (2009)
17. F. Siewert, R. Reininger, M. Rübhausen, "A KB-Focusing Mirror Pair for a VUV-Raman Spectrometer at FLASH-Mirror Metrology and Ray Tracing Results", AIP Conference Proceedings **1234**, 752-755, (2010)
18. S. Kalbfleisch, M. Osterhoff, K. Giewekemeyer, H. Neubauer, S.P. Krüger, B.. Hartmann, M. Bartels, M. Sprung, O. Leupold, F. Siewert, and T. Salditt, "The holography endstation of beamline P10 at PETRA III", AIP Conference Proceedings **1234**, 433-436, (2010)
19. L. Samoylova, H. Sinn, F. Siewert, H. Mimura, K. Yamauchi, T. Tschentscher, "Requirements on hard x-ray grazing incidence optics for European XFEL: analysis and simulation of wavefront transformations", Proc. of the SPIE, **7360**, 1-9 (2009)
20. P. Kirkpatrick and A.V. Baez, "Formation of Optical Images by X-Rays", JOSA, **38** (9), (1948)
21. Sébastien Boutet1 and Garth J Williams, "The Coherent X-ray Imaging (CXI) instrument at the Linac Coherent, Light Source (LCLS)", New Journal of Physics **12**, 035024, (2010)
22. F. Siewert, H. Lammert, T. Noll, T. Schlegel, T. Zeschke, T. Hänsel, A. Nickel, A. Schindler, B. Grubert, C. Schlewitt, "Advanced metrology, an essential support for the surface finishing of high performance x-ray optics", in "Advances in Metrology for X-Ray and EUV Optics", Ed. By Lahsen Assoufid, Peter Z. Takacs, John S. Taylor, Proc. of SPIE **5921,** 1-14 (2005)
23. S.C. Irick, Rev. Sci. Instrum. **63**(1), 1432-1435 (1992)
24. R. Signorato, M. Sanchez del Rio, "Structured slope errors on real x-ray mirrors: Ray tracing versus Experiment", Proc. of SPIE, **3152**, 136-147 (1997)
25. F. Siewert, "Slope Error and Surface Roughness", in: Modern Developments in X-ray and Neutron Optics, Springer, 175-179 (2008)
26. A. Rommeveaux, L. Assoufid, H. Ohashi, H. Mimura, K. Yamauchi, J. Qian, T. Ishikawa, C. Morawe, A.T. Macrander, A. Khounsary, S. Goto, "Second metrology round-robin of APS, ESRF and SPring-8 laboratories of elliptical and spherical hard-x-ray mirrors", Proc. of SPIE **6704**, 67040B, 1-12 (2007)
27. D. Cocco, G. Bartoletto, R. Sergo, G. Sostero, I. Cudin, "A hybride active optical system for wave front preservation and available focal distance", Nucl. Instrum. Meth. A **616,** 128-133, (2010)
28. M. Born, E.Wolf, "Principles of Optics", 7th ed. Cambridge University Press, Cambridge (1999).
29. J. C. Wyant, K. Creath, "Basic Wavefront Aberration Theory for Optical Metrology", Applied Optics and Optical Engineering, Vol. XI, Chap. 1,R. Shannon and J. C. Wyant, eds., Academic Press, Boston, MA, (1992)
30. A. Maréchal, Revue d'Optique, Theorique et Instrumentale **26**, 257 (1947)
31. T. Kimura, H. Ohashi, H. Mimura, D. Yamakawa, H. Yumoto, S. Matsuyama, T. Tsumura, H. Okada, T Masunga, Y. Senba, s. Goto, T. Ishikawa, nK. Yamauchi, "A stitching fugure profiler of large X-ray mirrors using RADSI for subaperture data acquisition", Nucl. Instrum. Meth. A **616,** 229-232 (2010)
32. K. Yamauchi, H. Mimura, K. Inagaki and Y. Mori, "Figuring with subnanometer-level accuracy by numerically controlled elastic emission machining", Rev. Sci. Instrum., **73** (11) (2002)
33. K. Yamauchi, K. Yamura, H. Mimura, Y. Sano, A. Saito, K. Ueno, K. Endo, A. Souvurov, M. Yabashi, K. Tamasaku, T. Ishikawa, Y. Mori, "Microstitching interferometry for x-ray reflective optics", Rev. Sci. Instrum **74**(5), 2894-2898 (2003)
34. J.C. Wyant, "White light interferometry", Proc. of SPIE **4737**. 98-107 (2002)
35. E.L. Church and P.Z. Takacs, "Specification of surface figure and finish of X-ray mirrors in terms of system performance", Appl. Opt.. **32**(19), 3344-531 (1993)
36. E.L. Church and P.Z. Takacs, "Specification of glancing- and normal-incidence X-ray mirrors", Optical Eng. **34**(2), 353-60 (1995)
37. V. Yashchuk, E. Gullikson, M. Howells, S. Irick, A. MacDowell, W. McKinney, F. Salmassi, T. Warwick, J. Metz, T. Tonnessen, "Surface roughness of stainless-steel mirrors for focusing soft x rays", Appl. Opt., **45**(20), 2006

38. M. Bowler, F. Siewert, B. Faatz, K. Tiedtke, "Investigating the effect of mirror imperfections in photon transport systems for FEL`s", Proceedings of the FEL2009, Liverpool, UK (2009)
39. V. Yashchuk, "Optimal measurement strategies for effective suppression of drift errors", Rev. Sci. Instrum., **80**, 115101 (2009)

1. Introduction

Transport and focusing of photons from a hard X-ray Free Electron Laser (FEL) to an experimental station on a length scale of a few hundred meters is a challenging task as it can result in a significant loss of brilliance and coherence. It requires X-ray optics with optical elements of utmost accuracy. The challenge is extreme for reflective focusing optics as such mirrors should be as long as possible and yet meet the minimum residual figure error requirement. This pushes both optics fabrication (polishing) and associated metrology verification to the very limits of currently available technology. Equally important to mirror polishing quality is manufacturing of a stress-free mount capable of integrating such optics with their high stability positioning system working in UHV environment. The mounting of such ultra-precise optical elements in their holders and in their working geometry is critical as it limits the beamline performance. Thus, the characterization of the optical elements in both the free and the mounted state and in their nominal configuration is of uttermost importance to enable a shape-preserving installation.

Since the late 1980's, the use of slope measuring instruments has become a standard technique to measure the long spatial frequency error (LSFE) of optical elements to be used under grazing incidence in synchrotron radiation applications [1,2,3]. First generation instruments such as the Long Trace Profiler (LTP) [3,4] and, for the last few years, 2nd generation slope measuring profilers like the Nanometer Optical Component Measuring Machine (NOM) [5,6,7,8] or the ESAD-method [9,10] enable the inspection of long, reflective free-form surfaces by direct measurement of the deflection angle of a laser beam along the line of inspection. The BESSY-NOM is a hybrid of a LTP-III-head [5,6] and a special autocollimator utilizing a very small aperture of 2mm [5,6]. Previous investigations demonstrated its ability to measure plane and slightly curved optics with a precision of 0.05µrad rms [11]. A careful characterization and calibration of the sensor is mandatory to achieve the required measurement performance [12,13,14]. This type of extremely accurate metrology instrumentation is essential for a detailed characterization of upcoming high performance reflective optical elements like long ultra-flat dynamically bendable mirrors for FEL application [15], diffraction limited focusing optics [16] as well as for the inspection in the mounted state of X-ray optics to guarantee a shape-preserving installation at the beamline. Furthermore, the obtained data enables realistic simulations to check the expected beamline performance [17,18,19]. In the present case, a Kirkpatrick-Baez (KB) focusing pair [20], with both mirrors shaped as plano-elliptical cylinders for the Coherent X-ray Imaging (CXI) instrument at LCLS [21] was measured in the free and mounted states and in their effective working geometry.

2. Measurement of slope deviation by use of the BESSY-NOM-autocollimator

Slope measuring systems enable the inspection of reflective surfaces by direct measurement of the deflection angle of a probing laser beam. Their advantage over interferometric system is that they do not rely on external reference surfaces. In the case presented in this paper we used the NOM-autocollimator to carry out the overall figure measurements of both mirrors. The NOM-autocollimator has been shown to provide a higher accuracy compared to the LTP-III-head of the NOM [22]. A laser test beam is traced at regular intervals over the mirror along the line of inspection. Depending on the local topography, the test beam will be reflected into the position sensitive detector of the NOM autocollimator head. Its position on the CCD-line of the sensor is directly related to the local surface slope, see Fig. 1. The reflection of the test

beam along the optical axis of the instrument is determined by the angle θ between the mirror normal and the direction of the impinging laser beam [23,24,25]. Then the local slope S is given by:

$$S(x) = \tan\theta = dy / dx \tag{1}$$

The relative slope change is measured by scanning along the line of inspection. The sensor detects the change of the angle of reflection from one position x on the mirror substrate to the next position x + Δ x. Figure 1 shows the optical setup for the scanning penta-prism. configuration by use of an autocollimator as sensor at the NOM. A diaphragm placed at a distance of 3mm from the optics under test defines the size of the measuring beam. A spatial integration of the slope data finally gives the topography profile $h(x_k)$:

$$h(x_k) = h(x_0) + \sum_{m=1}^{k} \frac{dx}{2}\left[S(x_m) + S(x_{m-1})\right] \tag{2}$$

The residual figure error is obtained after the subtraction of an ideal profile, given by an elliptical fit [26] based on the geometrical parameters as defined by the experimental setup. When using an aperture size of 2mm at the diaphragm the spatial period range covered by NOM is from 2mm to the full mirror length. Virtually any curved, reflective optical shape can be measured by the NOM as long as the slope change is within a ± 5mrad acceptance angle.

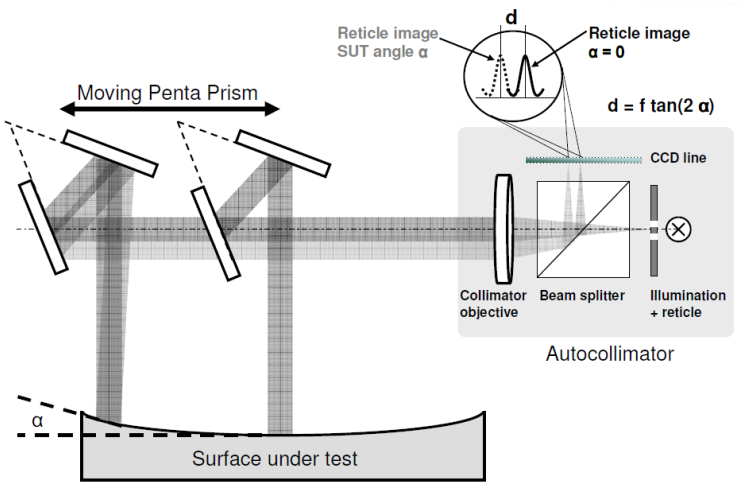

Fig. 1. principle set-up of a mirror based moving penta prism slope measuring profiler as realized for the BESSY-NOM

A larger slope change along a line of inspection can be measured by use of stitching techniques as long as the local curvature of the surface under test is not stronger than about 5m.

The double CCD array setup of the autocollimator provides a two-axis angle coordinate system (horizontal and vertical) which allows a measurement of a surface under test in face to the side or face up condition by use of the second CCD-array at the same optics head; only a simple change in the beam guiding mirror based penta prism (MBPP) setup is required. This option is realized at the NOM by a dedicated horizontal MBPP which must be aligned at the

scanning carriage in order to change the scanning beam path from a vertical to a horizontal reflection, thus allowing to characterize the two mirrors used in a classic KB setup (herafter named Horizontally and Vertically Focusing mirror, HFM and VFM, respectively) in their real operating conditions concerning the relative orientation of the optical surface versus gravity.

3. Ultra-precise diffraction-limited elliptical focusing mirrors – requirements and characterization

The impact of mirror shape imperfections in the long spatial frequency error (from about 1mm to aperture length) on the imaging performance of an X-ray focusing system is related to the induced local phase shifts in the reflected beam which distort the wavefront and cause the converging beam to have phase errors. This produces an imperfect wave overlap at the focal plane, see Fig. 2. A shape deviation of Δh on the aperture will have an influence on the wavefront of a phase φ described as follows:

$$\varphi = \frac{2\Delta h \sin\theta}{\lambda} \tag{3}$$

with θ being the angle of incidence and λ the wavelength of the X-ray beam [27].

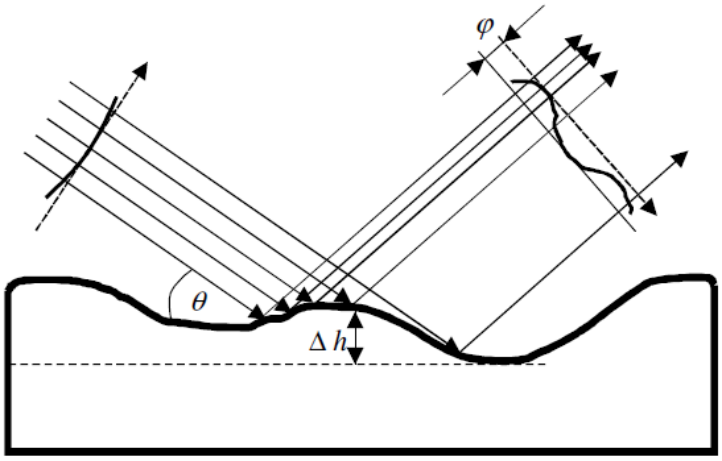

Fig. 2. Wave front distortion caused by shape deviations on an imperfect mirror

A further approach to describe the influence of shape imperfections is given by the Strehl ratio, as it is universally accepted as a measure of the quality of an optical system [28]. For small wavefront distortions the Strehl ratio can be approximated as [29]:

$$\frac{I}{I_0} \approx \exp\left[-\left(\frac{2\pi\sigma_{rms}}{\lambda}\right)^2\right] \qquad (4)$$

with $\frac{I}{I_0}$ for the ratio between the achieved peak intensity of the real optic and the ideal peak intensity of a perfect optical system. σ_{rms} is the root mean square wavefront distortion in units of length. A Strehl ratio of 0.8 or larger is generally accepted within the X-ray community as the measure of a high quality condensing optical system as it is associated with systems where 80% of the incoming light is found within the central intensity maximum at the focal plane. Using the calculated phase shift of the reflected light by an imperfect optical surface allows one to calculate the surface quality required in order to meet the Strehl ratio criterion of 0.8 which represents an rms wavefront distortion $\sigma_{rms} < \lambda$ /14. This leads to a condition known as the Maréchal criterion [30] where the root mean square height error over all spatial frequencies present within the residual surface errors is given by h_{rms}.

$$\Delta h_{rms} \leq \frac{\lambda}{14\sqrt{N}\,2\theta} \qquad (5)$$

where N is the number of reflecting surfaces in the system and θ is once again the angle of incidence of the beam being reflected off this surface. Clearly, the requirements on surface quality become linearly more difficult to achieve with decreasing X-ray wavelength, hence the difficult challenge of making hard X-ray reflective optics of the necessary quality. In the case of the CXI instrument, this condition lead to a h_{rms} <1.1 nm figure error requirement at a photon energy of 11 keV, if a single reflecting optic is present in each direction. However, as described in [21], a set of offset mirrors is always present in the front end of LCLS and there is a total of 3 reflective optics always present in the horizontal (2 offset mirrors and 1 KB mirror). Only one reflective optic is present in the vertical direction. With 3 optical elements in the beam path, the height error requirement becomes as stringent as h_{rms} <0.7 nm on all the optical surfaces at 11 keV. This is an extreme specification for elliptical mirrors of 350 mm length. It is noted here that diffraction limited focussing mirrors manufactured in the past usually had a useful aperture length of less than 100mm. Only recent improvements in metrology and finishing technology made the finishing of the CXI mirrors possible [31]. A specification of h_{rms} <1 nm was deemed achievable when the order for the CXI KB mirror substrates was placed and was thus requested to the optics manufacturer (JTEC Corporation, Osaka, Japan). Bruker ASC GmbH was responsible for the complete design, procurement, manufacturing, integration and testing of the KB system, including optics, UHV mirror holders and positioning mechanics, vacuum system and overall high-stabilizy support. The energy of 11 keV is used here to define the Maréchal criterion since it represents the high energy cutoff of the reflectivity of the CXI KB when coated with SiC, as specified with a 3.4 mrad incidence angle for these mirrors. The CXI instrument is expected to operate primarily in the 4 to 10 keV range when using these KB mirrors. The beam delivered by the LCLS undulators will range in size between 0.75 mm and 2 mm depending on the photon energy when it reaches the CXI mirrors. With the mirrors located 420 m away from the source, a demagnification of the source by a factor of 50 is expected to produce a ~ 1.5 micron focus at the sample. The collection efficiency of the mirrors is expected to be above 50%, with some

losses coming from the overfilling of the 1.18 mm aperture by the larger beam at lower photon energies. The collection efficiency decreases for lower energy, due to a larger beam caused by larger divergence. Each pulse of the LCLS will have approximately 2 mJ of energy delivered in 50 fs or less.

The two elliptical cylinder shaped focusing mirrors under discussion here were manufactured by use of elastic emission machining (EEM) – a deterministic surface finishing technology [32], developed at Osaka University, Japan. Interferometric sub-aperture stitching metrology [33] was applied by the manufacturer to control the level of figure accuracy achieved during the different steps of deterministic polishing and for the final acceptance tests. The task of the verification in Berlin was to give an independent third-party cross-check of the mirrors shape by use of a different measuring method. Slope measuring deflectometry was used to investigate the shape of the mirrors as delivered by the manufacturer and subsequently to assess the influence of the mirror mount (holder) on the final shape. The aperture for these grazing incidence KB mirrors is 350mm long in meridional direction, while in the sagittal direction only 1-2 mm of the aperture width is used. Thus, a line-scan along the long axis of the mirror allows one to obtain adequate information on the mirror state for the LSFE. The radius of curvature of the two mirrors is ranging from about 4 to 5 km, thus the used angular range on the autocollimator detector is small, about ±35 µrad only and the impact of inherent systematic error sources coming from the instrument itself is very limited [11]. The higher spatial frequency error part was measured in another set of measurements, by use of a White Light Interferometer (WLI), with magnification 2.5x and 20x applied. WLI measurements are a well known standard technique to inspect this part of the figure error budget and thus will not further be discussed here [34] (for the measured values see Table 1 and 2).

Due to the extremely challenging requirements for the residual figure error of 1nm rms for the optics in the mounted state, the mirrors were measured under three different conditions (see also Tab.1 and 2 for the detailed mirror specification). First both mirrors were supported by a cloth on a flat surface, providing full contact to the underside of the optic with evenly distributed loads. Then the mirrors were placed in their respective mechanical holders and measured in the free (mirrors simply resting on three spherical support points located at the Bessel points) and clamped (with all contact point between the mirror and the holder fully locked) state, in face up condition for the vertically focusing mirror (VFM) and face to the side for the horizontally focusing mirror (HFM), see Fig. 3.

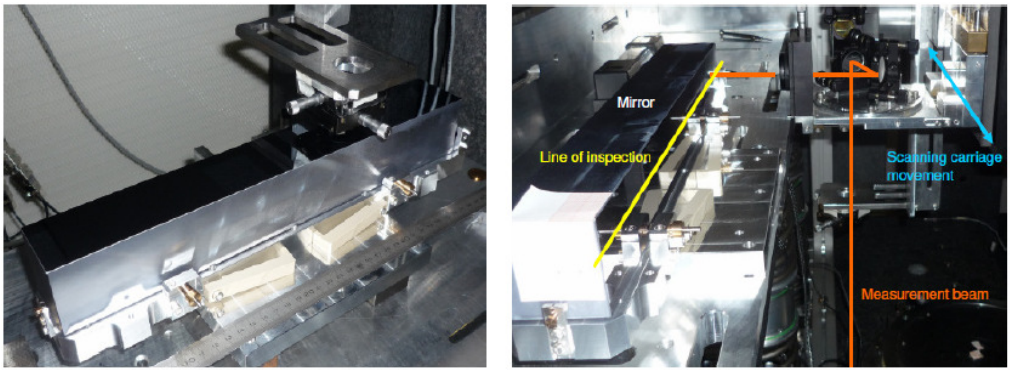

Fig. 3. left: - the VFM in the mounted state in face up position during measurement; right: - the HFM in the mounted state during measurement in face to the side condition.

4. Measurement results

The measurement results show that both mirrors are fully compliant with the specifications in the mounted state, see Table 1 and 2. In case of the HFM no significant change of the mirror shape occurred comparing the face up (on a cloth) and the face to the side state, see Fig. 4 and 5. The residual figure error is 0.57 nm rms / 2.5 nm pv for the free standing (cloth-supported) and face up state. While the mounted state in face to the side condition shows 0.68 nm rms / 2.8 nm pv.

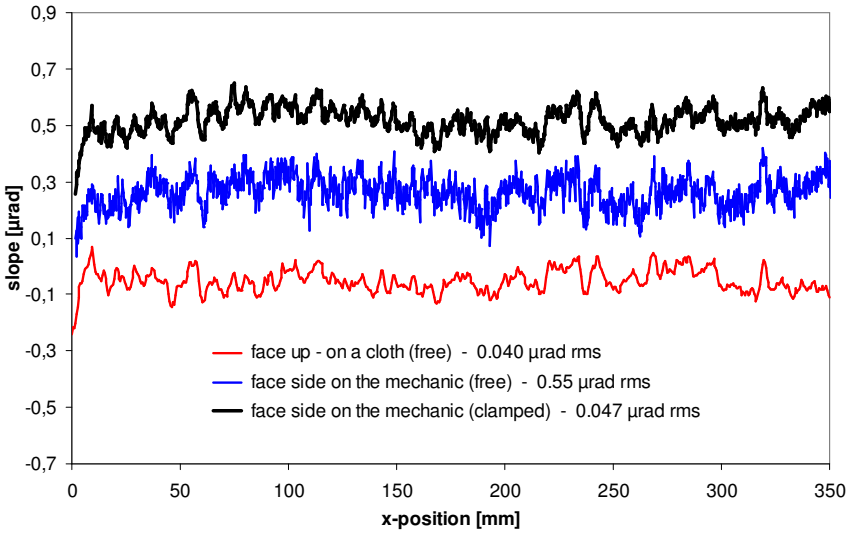

Fig. 4. HFM profiles of residual slope error after subtraction of a best fit ellipse for free state face up and face to side state free and clamped in the mechanics. The measurement in the face up state was performed with dx = 0.5 mm increments, averaging 20 scans forward and backward. The measurements in face to side condition were performed with dx = 0.2 mm increments, averaging 12 scans in the free state and 39 scans forward and backward in clamped state. For better visualization a shift was added to the profiles of the face to side measurements.

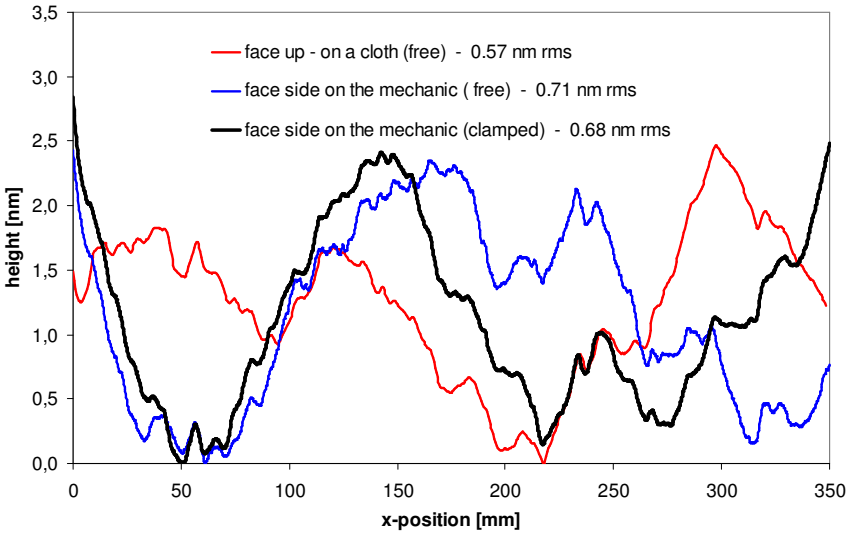

Fig. 5. Mirror HFM profiles of residual height corresponding to the profiles of residual slope shown in Fig. 4.

These values correspond to a residual slope error of 0.056 µrad rms (free) and 0.047 µrad rms (in the mounted state). To achieve a residual figure error of < 1nm rms the VFM got a dedicated pre-figuring to compensate the deformation of the mirror blank caused by gravitation under the designed mechanical support scheme. For the VFM a change in the order of a factor of 2 for the residual figure error can be considered due to gravity alone. The free state (cloth-supported) of the VFM in the face up measurement shows a residual figure error of 1.8 nm rms, see Fig. 6. Then a figure error of 0.9 nm rms was found in the mounted state (mirror supported at the Bessel points), face up in the mechanical holder. The corresponding values for the residual slope error are 0.066 µrad rms (free) and at 0.061 µrad rms in the mounted state, see Fig. 7. A more sophisticated option to evaluate the quality of the surface finishing is to transform the obtained height profiles into a one dimensional PSD [35,36,37]. Figure 8 shows the PSD-curves for the HFM and the VFM (in the mounted state) in comparison with the PSD-curve of an ellipsoidal focussing mirror manufactured by classical polishing technology. This mirror is characterized by a residual slope error of about 1.5 µrad rms on a length of 490 mm [38] – for the PSD comparison a reduced section of 350mm in length was chosen. The classical polishing causes a characteristic fingerprint of certain spatial frequencies like in the range of 3-5 mm and of further longer spatial frequency too (e.g. some 10 mm - see Fig. 8). The curves for the HFM and the VFM demonstrate that these specific shape deviations do not appear due to the deterministic surface finishing applied. In the case of the VFM a further cross check along the line of inspection was carried out to validate the reproducibility of the measurement as well as the achieved accuracy of the residual slope. The mirror was measured face up in the clamped state along the centre line in upstream – downstream and after a 180° horizontal flipping in downstream – upstream direction. Comparing the achieved results an agreement of 0.04 µrad rms was found. This value can be assumed as the estimated accuracy for the measured residual slope deviation. The contribution of random noise in both measurements is at approximately the same level. Thus, both measurements can be averaged, which allows to suppress parts of the systematic error on the measurement [39], and a residual slope error of 0.056 µrad rms can then be achieved for the VFM in the clamped state (see also Table 2).

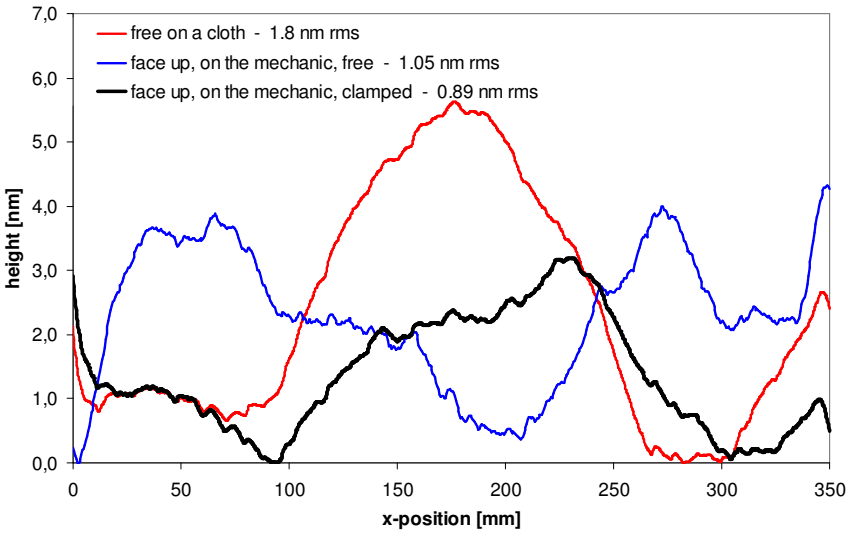

Fig. 6. VFM - profiles of residual height for the free state on a cloth and the free and clamped state in the mechanics at the centre line of the useful aperture.

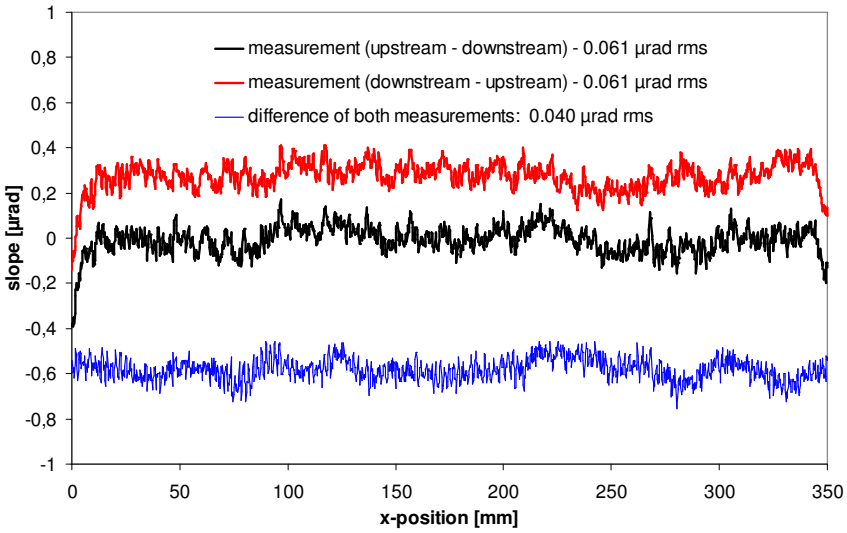

Fig. 7. VFM profiles of residual slope in the clamped state in the mechanic (face up condition). The measurements were taken in upstream – downstream and downstream – upstream direction at the centre line of the aperture. The agreement of both measurements is 0.04 µrad rms For better visualization a shift was added to the downstream – upstream measurement and the plot of the difference.

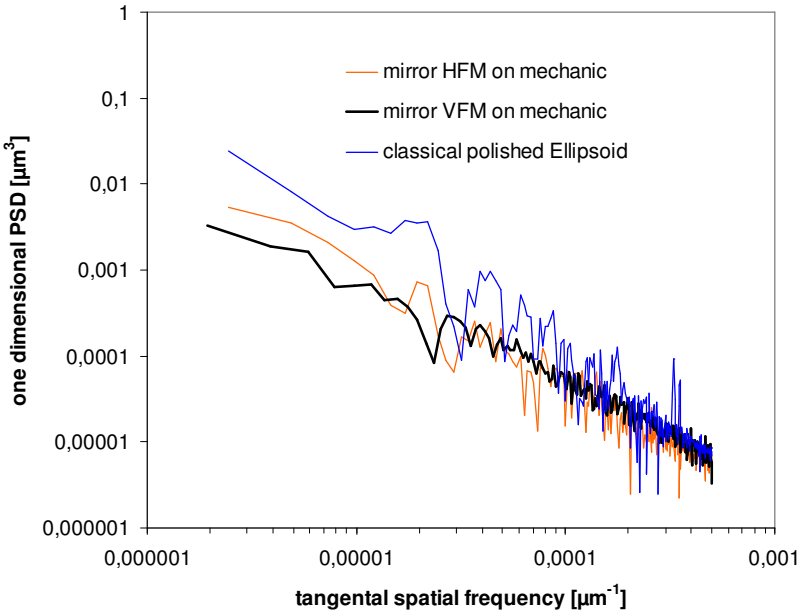

Fig. 8. Comparison of 1-dimensional PSD curves for the HFM and VFM made by EEM finishing technology (measurements for the state on the mechanic) with an ellipsoidal focussing mirror made by classical polishing technology.

Table 1. Shape parameter of the HFM elliptical cylinder mirror, as measured by use of NOM and WLI[a].

HFM parameter	Specification	Measurement result
Source distance r [mm]	420000 ± 20000	420000
Focus distance r` [mm]	8700	8700
Incidence angle θ [mrad]	3.3663	3.352
Residual slope error [μrad rms]	0.25	0.040 (free) / 0.047 (clamped)
Residual figure error [nm rms]	< 1.0	0.57 (free) / 0.68 (clamped)
MSF Roughness [nm rms]	≤ 0.25	0.14 – 0.25
HSF Roughness [nm rms]	≤ 0.25	0.19

[a]The MSF and HSF was measured by use of a Micromap Promap white light interferometer (WLI) using magnification 10x, and 50x, all other results are based on NOM measurements.

Table 2. Shape parameter of the VFM elliptical cylinder mirror, as measured by use of NOM and WLI[b].

VFM parameter	Specification	Measurement result
Source distance r [mm]	420000 ± 20000	420000
Focus distance r` [mm]	8300	8300
Incidence angle θ [mrad]	3.3647	3.359
Residual slope error [μrad rms]	0.25	0.066 (free) / 0.056 (clamped)
Residual figure error [nm rms]	< 1.0	1.83 (free) / 0.89 (clamped)
MSF Roughness [nm rms]	≤ 0.25	0.14 – 0.16
HSF Roughness [nm rms]	≤ 0.25	0.04 – 0.05

[b]The MSF and HSF was measured by use of a Micromap Promap white light interferometer (WLI) using magnification 10x, and 50x, all other results are based on NOM measurements.

5. Shape preservation and mechanical mounting of optical elements – a critical issue

In the case of ultra precise optical elements their mechanical holder and clamping could easily cause system performance limiting shape deformations. Our measurements have shown that even a minor change in the mirror shape can be detected after fastening the clamping screws (see Fig. 5 and 6). This important issue needs to be to considered and kept strictly under control for a shape preserving installation of such high performance optical elements at a beamline in general.

To demonstrate this problem we report a test measurement of the VFM. Figure 9 shows a comparison of different states of the mirror as inspected by use of the NOM. Our measurements clearly show that at the extreme level of accuracy of these optics, inappropriate clamping forces can easily cause a significant shape deformation, see Fig. 9 (for this demonstration the same ellipse fit parameters were used as for the final mounted state). In this specific case the specified acceptable figure error of $h_{rms} < 1$ nm would clearly not be met

with excessive meridional clamping forces applied. This represents a simple but eplicit demonstration that optics and mechanics together have to be understood and tested as a unit. Thus the mounting supported by precise metrology instrumentation is mandatory.

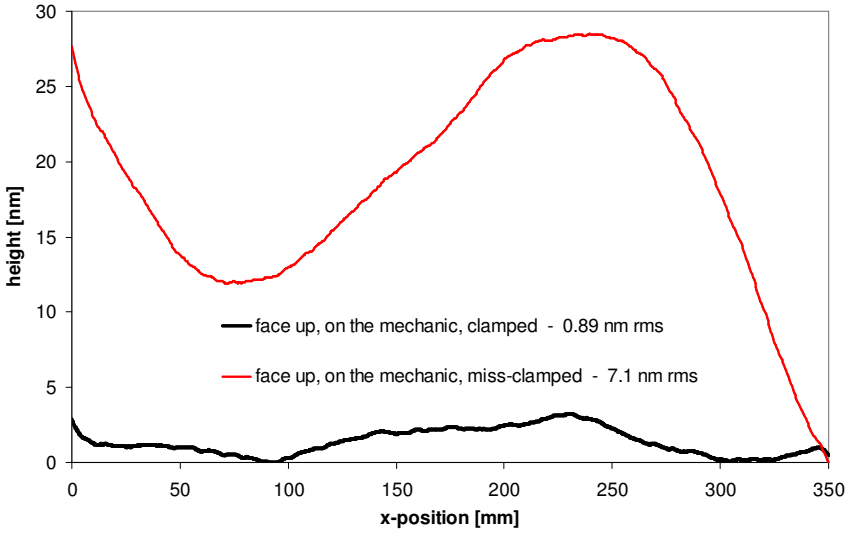

Fig. 9. VFM – profiles of residual height for the free in the mechanic and clamped in the mechanic state – showing the impact of miss-clamping in meridional direction

6. Concluding remarks

The results presented here have shown that even extreme requirements for diffraction limited focusing optics such as < 1nm rms figure error are realistic to be manufactured and, very importantly, can also be obtained with the mounted optics. Deterministic surface finishing technology allows to provide sub-nanometer rms accuracy on the entire range from low to high spatial frequency for mirrors up to 350mm in length.

High resolution slope measuring deflectometry allows accurate inspection of ultra-precise optical elements in the free state as well as in the mounted state with sub nm accuracy. Optical elements can be inspected for both orientations, in the face up and face to the side condition if an autocollimator and an adaptive based penta prism (MBPP) are used to perform slope measurements.

It was shown that gravitational effects on the mirror shape can be compensated if advanced metrology and deterministic surface finishing technique is applied to figure the mirror shape. The clamping of optics was shown to be a critical step for the final installation of such optics. A mis-clamping could cause changes in the range of the long spatial figure error. This can be easily identified by NOM slope measurements and thus optimized.

Acknowledgements

This work was partly funded by the LCLS Ultrafast Science Instrument (LUSI) major item of equipment project, which provided funding from the U.S. Department of Energy – Basic Energy Science for the construction of three hard X-ray instruments at LCLS. Portions of this

research were carried out at the Linac Coherent Light Source (LCLS) at the SLAC National Accelerator Laboratory. LCLS is an Office of Science User Facility operated for the U.S. Department of Energy Office of Science by Stanford University.

Design, procurement, manufacturing, testing and installation of the CXI KB1 system has been fully performed by Bruker ASC GmbH, in the framework of subcontract 80060 issued by the Leland Stanford Jr. University, Menlo Park, CA.

The authors would like to thank JTEC Corp., Kobe, Japan for excellent work on the mirror finishing.